Theory of tunneling spectroscopy in UPd_2Al_3

David Parker[1] and Peter Thalmeier[2]
[1]*Max Planck Institute for the Physics of Complex Systems, Nöthnitzer Strasse 38, D-01187 Dresden, Germany*
[2]*Max Planck Institute for the Chemical Physics of Solids, Nöthnitzer Strasse 40, D-01187 Dresden, Germany*
(Received 18 December 2006; revised manuscript received 30 January 2007; published 2 May 2007)

There is still significant debate about the symmetry of the order parameter in the heavy-fermion superconductor UPd_2Al_3, with proposals for $\cos(k_3)$, $\cos(2k_3)$, $\sin(k_3)$, and $e^{i\phi}\sin(k_3)$. Here, we analyze the tunneling spectroscopy of this compound and demonstrate that the experimental results by Jourdan *et al.* [Nature (London) **398**, 47 (1999)] are inconsistent with the last two order parameters, which are expected to show zero-bias conductance peaks. We propose a definitive tunneling experiment to distinguish between the first two order parameters.

DOI: 10.1103/PhysRevB.75.184502 PACS number(s): 74.20.Rp

I. INTRODUCTION

Superconductivity in UPd_2Al_3 with a transition temperature $T_c=2$ K was discovered in 1991 by Geibel *et al.*,[2] and since that time much experimental and theoretical work has been performed, with a particular aim of establishing the order-parameter symmetry. In general, this determination is a crucial first step in understanding the pairing mechanism of a given superconductor, so that much effort is generally expended in this direction.

Evidence for unconventional or nodal superconductivity in UPd_2Al_3 has emerged from a variety of experiments. Feyerherm *et al.*[3] measured the Knight shift in UPd_2Al_3 and found a substantial reduction below T_c, indicative of singlet pairing. In NMR experiments, Tou *et al.*[4] and Matsuda *et al.*[5] found low-temperature nuclear spin lattice relaxation rate T_1^{-1} power law (T^3) behavior and the absence of a Hebel-Slichter coherence peak below T_c. Both behaviors are characteristic of nodal superconductivity, and in particular, the observation of T^3 behavior is strongly suggestive of line nodes in the order parameter. Similar evidence was obtained by Geibel *et al.*,[2] who measured the low-temperature specific heat and found T^2 behavior, also indicative of line nodes. Hiroi *et al.*[6] measured the low-temperature thermal conductivity and also found T^2 behavior. More recently, Watanabe *et al.*[7] measured the angle-dependent magnetothermal conductivity and found evidence for a single line node parallel to the basal plane of the hexagonal UPd_2Al_3.

Tunneling spectroscopy can be a powerful probe of order-parameter symmetry. The pioneering work in this field was performed by Blonder, Tinkham, and Klapwijk (BTK),[8] who provided a simple solution to the problem of Andreev reflection[9] in *s*-wave superconductors in an N-I-S contact, and by Tanaka and Kashiwaya,[10] who were able to explain the zero-bias conductance peaks (ZBCPs) generally observed in tunneling measurements of the high-temperature cuprate superconductors.[11] Since that time, much theoretical work on tunneling spectroscopy in various materials has been performed; primary references of interest are the book by Tinkham[12] and the study by Honerkamp and Sigrist.[13]

The basic conclusion of the original work of Tanaka and Kashiwaya was that zero-bias conductance peaks are intimately tied in with the phase difference between the pair potentials of the transmitted electronlike and holelike quasiparticles on the superconducting side of the junction. When this phase difference reaches π, Andreev reflection (resulting in the transmission of two electrons for a single incoming electron) is enhanced and normal reflection diminished, so that the transmission coefficient is increased. This enhancement is most prominent at zero energy. At increasing tunneling energy barrier height (the thin oxide layer between the superconductor and normal), the normal-state conductance decreases, so that the relative conductance, or the ratio of superconducting to normal-state conductance, increases. It should be noted that while strongly enhanced ZBCPs (diverging in the limit of large barrier height) only result from a π phase difference, significant zero-energy states can be realized in other cases, as in Ref. 13. We show below that for the case of interest, substantial amounts of zero-energy states can be realized even for order parameters without the requisite π phase change, when the effects of impurity scattering are accounted for. The magnitude of these zero-energy states, as well as the height and energy of the quasiparticle coherence peaks, is a strong function of the order parameter, and for the geometry appropriate to UPd_2Al_3, of the normal metal used in the junction, so that a wide range of interesting and informative experimental results can be obtained, offering a definitive resolution to the question of order-parameter symmetry in UPd_2Al_3.

II. MODEL

In general, the pair state of a superconductor is described by the Bogoliubov-deGennes equations:[8,10,14,15]

$$i\hbar\frac{\partial f}{\partial t} = -\left[\frac{\hbar^2\nabla^2}{2m} + \mu + V(x)\right]f(\mathbf{x},\mathbf{k},t) - \Delta(\mathbf{x},\mathbf{k})g(x,t), \tag{1}$$

$$i\hbar\frac{\partial g}{\partial t} = \left[\frac{\hbar^2\nabla^2}{2m} + \mu + V(x)\right]g(\mathbf{x},\mathbf{k},t) - \Delta(\mathbf{x},\mathbf{k})f(x,t). \tag{2}$$

Here, as in Ref. 15, we take the f's as electron wave functions and the g's as hole wave functions, and note that the solutions to these equations can be written as

$$f(\mathbf{x},\mathbf{k},t) = u(\mathbf{k})\exp[i(\mathbf{k}\cdot\mathbf{r} - Et)/\hbar], \tag{3}$$

$$g(\mathbf{x},\mathbf{k},t) = v(\mathbf{k})\exp[i(\mathbf{k}\cdot\mathbf{r} + Et)/\hbar], \tag{4}$$

where u and v are the well-known BCS coherence factors:[13,15,22]

$$u(\mathbf{k}) = \sqrt{\frac{1}{2}(1 + \sqrt{E^2 - |\Delta^2(\mathbf{k})|}/E)}, \tag{5}$$

$$v(\mathbf{k}) = \sqrt{\frac{1}{2}(1 - \sqrt{E^2 - |\Delta^2(\mathbf{k})|}/E)}. \tag{6}$$

We note that in the initial BCS formulation, these u and v coefficients are only defined for $|E| > |\Delta(\mathbf{k})|$, but in this work we will extend this usage to energies $E < \Delta(\mathbf{k})$ including negative energy, and will incorporate into the model the effects of impurity-scattering-induced level broadening by adding an imaginary part Γ to the energy E.

A. Consideration of impurity scattering effects

In general, nonmagnetic impurities in the dilute limit in unconventional superconductors can be treated by the standard Abrikosov-Gor'kov theory[16] within the self-consistent T-matrix[17] approximation. The two limits usually cited and readily calculated are the Born limit (weak scattering) and the unitary limit (strong scattering), parametrized by the phase shift δ between incoming and scattered quasiparticles. Impurity effects in heavy-fermion superconductors are generally close to the unitary limit[18] with $\delta \sim \pi/2$ and we adopt this assumption here. Then, within the Abrikosov-Gor'kov theory the quasiparticle energy ω is renormalized as follows:

$$\tilde{\omega} = \omega + i\Gamma_{unitary}\left\langle \frac{\tilde{\omega}}{\sqrt{\tilde{\omega}^2 - \Delta^2 f^2}} \right\rangle^{-1}. \tag{7}$$

Here, f is not a Bogoliubov-deGennes electronlike wave function but rather contains the angular dependence of the order parameter, i.e., $\Delta(\mathbf{k}) = \Delta(T)f(\mathbf{k})$, and the expectation value indicates average over the Fermi surface. In the general case, there is a similar equation for the renormalized gap function $\tilde{\Delta}(\mathbf{k})$, but here for all order parameters under consideration the relevant Fermi-surface average vanishes so that Δ is not renormalized, other than a constant, energy-independent reduction due to the impurity scattering rate. For the rest of this section, we assume a cylindrical Fermi surface and take $f = \cos(ck_3)$. The normal-state quasiparticle scattering rate $\Gamma_{unitary} = n_i/(\pi N_0)$, where n_i is the concentration of impurities and N_0 the normal-state density of states at the Fermi level.

Once $\tilde{\omega}(\omega)$ has been solved for, one can easily evaluate the quasiparticle density of states; in particular, within the unitary limit one obtains a finite density of states at the Fermi level and a truncated coherence peak at $\omega = \Delta$. Both these effects are also achieved by simply adding a constant imaginary part to the quasiparticle energy ω in the usual expression for the quasiparticle density of states, as was done by Dynes *et al.*[19]

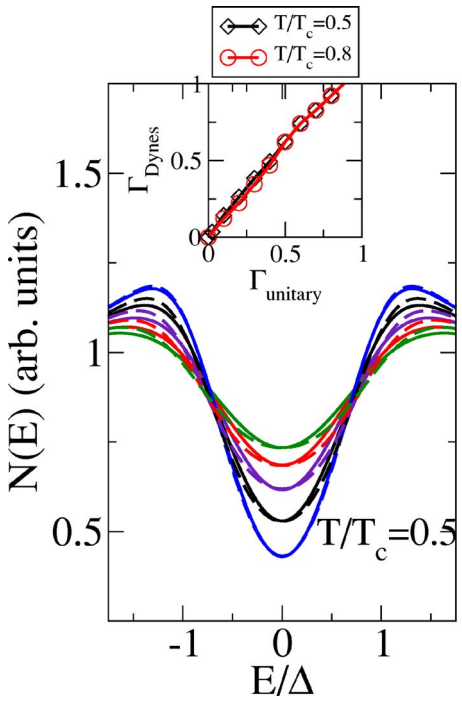

FIG. 1. (Color online) A comparison of the results for quasiparticle density of states using the Dynes formalism and unitary limit scattering is shown. From the bottom, the curves were calculated using (in units of Δ) $\Gamma_{unitary} = 0.025$, 0.1, 0.2, and 0.3, with the corresponding fit values of Γ_{Dynes} (inset).

$$N(\omega)/N_0 = \mathrm{Re}\left\langle \frac{\omega - i\Gamma_{Dynes}}{\sqrt{(\omega - i\Gamma_{Dynes})^2 - \Delta^2 f^2}} \right\rangle. \tag{8}$$

Note that ω is identical to the energy E introduced in the previous section; we are simply following the standard labeling convention. It is then natural to ask whether the rather complex calculational effects of resonant impurity scattering can be reproduced by the simpler Dynes formula. It turns out that this is indeed the case, when the effects of temperature broadening of the quasiparticle density of states are included. This temperature broadening is distinct from the impurity broadening effects discussed above, and can be expressed as

$$N_T(E) = \int_{-\infty}^{\infty} \frac{\beta dE'}{4} N(E')\mathrm{sech}^2[\beta(E - E')/2], \tag{9}$$

where $\beta = 1/kT$.

Figure 1 shows a comparison of the results for densities of states calculated using the full unitary limit calculation and the Dynes approximation at $T/T_c = 0.5$. The dashed lines indicate the unitary limit result, and the solid lines the Dynes approximation, for several values of impurity scattering $\Gamma_{unitary}$ and corresponding fit values of Γ_{Dynes}. The agreement is excellent, and we achieve similar agreement provided that the temperature is not too low ($T > 0.3T_c = 0.48$ K for UPd_2Al_3). This includes nearly all of the data of Jourdan *et al.* analyzed later in this work. Also of importance, the fitted values Γ_{Dynes}, as shown in the inset, are proportional to $\Gamma_{unitary}$, with a coefficient very near unity, and this coefficient is essentially temperature independent. For the purposes at

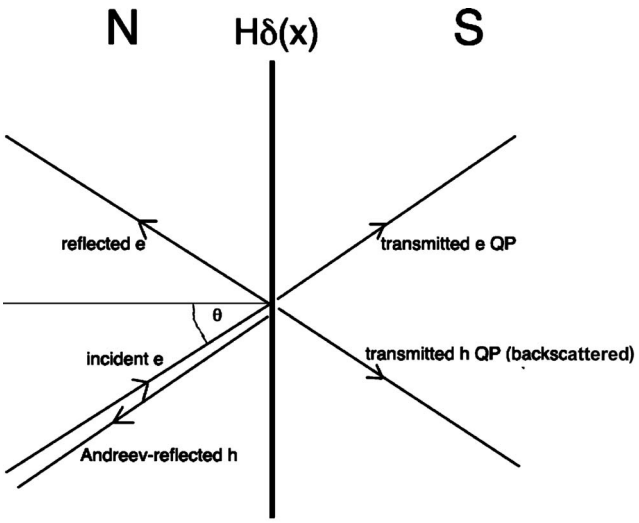

FIG. 2. A schematic diagram of all the particles involved in the reflection (transmission) process at a N-S boundary; the arrows indicate the direction of the group velocity. Note that for the holes the momenta are opposite to this direction.

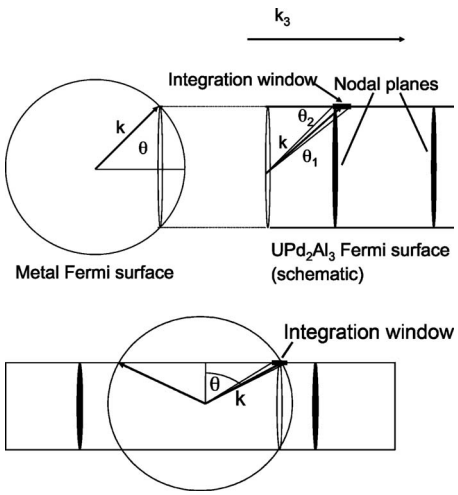

FIG. 3. A schematic diagram of the metallic and UPd_2Al_3 Fermi surfaces, for the longitudinal and transverse geometries. For the UPd_2Al_3 Fermi surface, we take the main cylindrical sheet (Ref. 26) and neglect its corrugation.

hand, then, the Dynes approximation is a good one, and the "quasiparticle scattering rate" Γ_{Dynes} is a good surrogate for the effects of resonant, unitary limit impurity scattering. We note that this Γ_{Dynes} originates from an entirely different source than the usual *inelastic* quasiparticle decay rate invoked in the modeling of tunneling density of states. As we shall see, this is sensible given that this decay rate is expected to be strongly temperature dependent,[20,21] while the modeling later in this paper shows a Γ_{Dynes} that is independent of temperature.

We note that other workers have previously applied the Dynes formalism to the problem of tunneling spectroscopy. Pleceník and co-workers[23,24] used this factor in order to model differential conductance in high-T_c cuprate-metal junctions, where substantial zero-energy density of states was observed, as is also true for the experimental data of Jourdan *et al.*[1] that will be analyzed later in this work.

B. Calculational considerations

With the coherence factors in place, we are now in a position to consider the process whereby an incident electron in a normal metal undergoes Andreev and normal reflection at the N-S interface, with an electronlike quasiparticle and a backscattered holelike quasiparticle transmitted. This process is depicted in Fig. 2. Note that the arrows indicate the particle group velocity; for the transmitted hole and Andreev-reflected hole, the momentum is opposite to this. We have included a delta-function potential $H\delta(\mathbf{x})$ to model the inclusion of a thin oxide layer between the superconducting UPd_2Al_3 and the normal metal. Translational invariance parallel to the interface dictates that the momentum in this direction be conserved, while the momentum perpendicular to the interface is also conserved in the approximation where the barrier energy is much less than the Fermi energy of the incoming electron.

We note that unlike in virtually all other studies of the tunneling spectroscopy of unconventional superconductors, the Fermi momentum of the normal metal plays a key role in selecting the wave vectors which will contribute to the conductance, as indicated in Fig. 3. Only a very small portion of the electrons in a spherical-Fermi-surface approximation will lie on the dominating, approximately cylindrical Fermi surface of UPd_2Al_3, as indicated, and therefore contribute to the superconducting or normal-state conductance. Electrons far from the Fermi-surface cylinder of the UPd_2Al_3 will play no role.

We will also see that the conductance results depend critically on whether the wave vector selected lies near a nodal line; thus, different metals used on the normal side can be expected to display radically different behaviors. Indeed, we will see that the measured gap magnitude, the zero-energy density of states, and even the existence of the usual coherence peaks will depend strongly on the metal used. Finally, we have corrected for the effects of the electron effective mass mismatch[25] at the interface.

III. CALCULATION METHODOLOGY

In our calculations, we follow the work of Blonder *et al.*,[8] Honerkamp and Sigrist,[13] and Tanaka and Kashiwaya.[10] The basic method is straightforward: apply the usual boundary conditions at the interface and solve for the amplitudes of the various components.

The incoming electron wave function can be written as

$$\begin{pmatrix} 1 \\ 0 \end{pmatrix} e^{ik_F x \cos\theta},$$

with θ the angle between the normal to the interface and $\mathbf{k}$. We have suppressed the part of the wave function depending on the momentum parallel to the interface, as due to the translational invariance in this direction all of the involved momenta are equal. On the normal-metal side, the Andreev-

reflected hole, with amplitude a, has wave function

$$\begin{pmatrix} 0 \\ 1 \end{pmatrix} e^{ik_F x \cos\theta},$$

and the normally reflected electron, with amplitude b, has wave function

$$\begin{pmatrix} 0 \\ 1 \end{pmatrix} e^{ik_F x \cos\theta}.$$

On the superconducting side, the electronlike quasiparticle, with amplitude c, has wave function

$$\begin{pmatrix} u(\theta) \\ \exp(-i\phi_\theta)v(\theta) \end{pmatrix} e^{ik_F x \cos\theta},$$

and the backscattered holelike quasiparticle has wave function

$$\begin{pmatrix} \exp(i\phi_{\pi-\theta})v(\pi-\theta) \\ u(\pi-\theta) \end{pmatrix} e^{-ik_F x \cos\theta}.$$

Here, the exponential factors represent the phase of the gap at the indicated angle. We are now able to apply the boundary conditions. Continuity of the wave function at the interface yields the first two of four equations for the four unknowns a, b, c, and d.

The usual boundary condition[8,10] appropriate for a delta-function potential $H\delta(x)$ is

$$\psi_S'(0) - \psi_N'(0) = \frac{2m}{\hbar^2} H\psi(0). \tag{10}$$

However, due to the large effective-mass mismatch at the boundary ($m_S \sim 100 m_0$), we must generalize this condition. Integrating the Bogolubov-deGennes equations across the boundary, we find

$$\frac{\psi_S'(0)}{m_S} - \frac{\psi_N'(0)}{m_N} = \frac{2}{\hbar^2} H\psi(0), \tag{11}$$

with the effective masses as indicated. We note that the substantial mass anisotropy of UPd_2Al_3 is contained entirely in the single m_S parameter, which at first glance appears incorrect. However, in the boundary-condition integration, only the longitudinal mass enters, and we therefore may use a single effective mass for UPd_2Al_3.

Substituting the wave functions outlined above into this formula leads to the final two equations for the four unknowns a, b, c, and d. We find the following solutions for a and b:

$$a(\theta,E) = \frac{uv}{D}, \tag{12}$$

with

$$D = (u^2 - e^{i(\phi_{\pi-\theta}-\phi_\theta)}v^2)|Z|^2 m + u^2, \tag{13}$$

$$b(\theta,E) = \frac{(u^2 - e^{i(\phi_{\pi-\theta}-\phi_\theta)}v^2)(|Z|^2 + Z)}{D}. \tag{14}$$

Here $m = m_S/m_N$ and $Z = H/(i\hbar v_F \cos\theta) + 1/2m - 1/2$, where v_F is the metallic Fermi velocity, and $e^{i\phi} = \frac{\Delta(\phi)}{|\Delta(\phi)|}$, i.e., the gap phase. The energy dependence of a and b is contained in the coherence factors u and v. We note two interesting effects.

(i) The denominator D increases rapidly with mass mismatch m and effective barrier height Z. There are therefore narrow transmission resonances when the prefactor of the $|Z|^2 m$ term vanishes. For all the order parameters under consideration, the factors u_θ and $u_{\pi-\theta}$ are identical, as are v_θ and $v_{\pi-\theta}$. When the phase factor is unity, i.e., there is no change of order-parameter sign under the change in angle from θ to $\pi-\theta$, the prefactor can only vanish when $u=v$, i.e., $E = \Delta(\mathbf{k})$. Thus, for the two cosine-containing order parameters, we expect coherence peaks in the differential conductance at the gap energy selected by the wave-vector matching on the UPd_2Al_3 Fermi surface. This implies that the energy, or voltage, of the conductance coherence peaks for these order parameters is a function of the normal metal's Fermi wave vector, in contrast to most tunneling spectroscopy studies, where no effects of wave-vector matching are considered, because the Fermi surface on the superconducting side is also considered spherical. It is the peculiar geometry engendered by the longitudinal Fermi surface of UPd_2Al_3 that creates this unusual coherence peak effect.

(ii) For the two sine-containing order parameters, the phase factor is -1, so that for a resonance we must satisfy $u^2 = -v^2$. Strictly speaking this is impossible, since $u^2 + v^2 = 1$, but the factors u and v diverge as $|E| \to 0$, so that both the numerator of $a(E,\theta)$ and the second term of D diverge, while the first term of D remains finite. As $E \to 0$, explicit calculation shows that for $\Gamma = 0$ we attain perfect transmission, and therefore, we expect zero-energy resonances to appear as zero-bias conductance peaks for these two order parameters.

Following BTK[8] and Tanaka and Kashiwaya,[10] the normalized conductance at temperature $T = 1/\beta$ is given by

$$dI/dV = \sigma(V) \equiv \frac{\sigma_S(V)}{\sigma_N(V)} = \frac{\int_{-\infty}^{\infty} dE \int_{\theta_1}^{\theta_2} d\theta \cos(\theta)\, \mathrm{sech}^2[\beta(E-V)/2](1 + |a(\theta,E)|^2 - |b(\theta,E)|^2)}{\int_{-\infty}^{\infty} dE \int_{\theta_1}^{\theta_2} d\theta \cos(\theta)\, \mathrm{sech}^2[\beta(E-V)/2]\sigma_N(E)}. \tag{15}$$

TABLE I. Metallic k_F and k_{z0} values.

Metal	k_F (10^8 cm/s)	k_F units of $(\pi/2c)$	k_z $(\pi/2c)$
Pb	1.58	4.21	3.88
Be	1.94	5.17	4.90
Al	1.75	4.66	4.37
Au	1.21	3.23	2.78
Ca	1.11	2.96	2.46

Note that we are not integrating over the full range of angles θ as the majority of such angles will result in wave vectors lying away from the nearly cylindrical[26] Fermi surface of UPd_2Al_3. In practice, what we have done in all cases is to use the metallic Fermi momentum to determine the angle at which this momentum lies on the UPd_2Al_3 Fermi surface and then computed k_{z0} (the component of this momentum along the Fermi surface). Values of metallic Fermi momenta and corresponding k_{z0} for the metals used in this paper, for the longitudinal geometry, are given in Table I.

We note that certain of the metals, such as Be and Au, have Fermi momenta causing the selected wave vector k_z to lie near a node of the $\cos(ck_3)$ order parameter, while Pb's k_z lies near an antinode, and we will see that this yields widely divergent behavior in the predicted tunneling conductances for these materials. Furthermore, Ca's k_z is very close to a node of the $\cos(2ck_3)$ order parameter, but relatively far from a node of the $\cos(ck_3)$ order parameter, so that these two order parameters would yield rather different predictions for a tunneling junction containing this metal, enabling an experiment to distinguish between these order parameters (discussed in Sec. VI).

As a rough accounting for actual metallic Fermi-surface deviations from spherical, we have integrated over angles corresponding to k_z from 0.95 to 1.05 k_{z0}. For alkali metals such as sodium,[36] this is an overestimation, while for other materials—such as tungsten—this understates the Fermi-surface deviations from spherical. Nevertheless, the results of our calculations are not sensitive to the size of the integration window used, provided that this window is small compared with the distance between the nodal planes. For all calculations, we have taken the effective-mass mismatch m as 100, while the barrier height H/v_F has been taken as unity. The results are not sensitive to either of these parameters.

IV. ORDER-PARAMETER PROPOSALS

Before presenting the results of our calculations, we give a brief summary of the order parameters which have been proposed for UPd_2Al_3. Note that in all proposals k_3 is taken as perpendicular to the ab plane, and c is the c-axis lattice constant.

Won *et al.*[29] proposed $\Delta(\mathbf{k})=\cos(2ck_3)$ based upon magnetothermal conductivity data,[7] while McHale *et al.*[27] performed a strong-coupling calculation and found that both $\cos ck_3$ and $\sin ck_3$ had the highest transition temperatures, among possible order parameters. It was noted[28] that the chiral order parameter $\exp(i\phi)\sin ck_3$, where $\exp(i\phi)=\hat{k}_1+i\hat{k}_2$, is also a possible candidate. All of these order parameters contain nodal lines perpendicular to the k_3 axis, which were found in magnetothermal conductivity[7] measurements on this material.

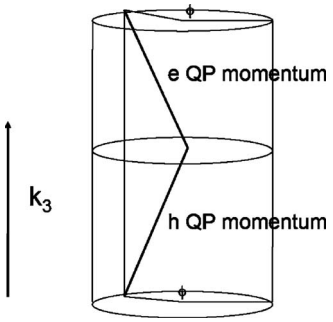

FIG. 4. A schematic diagram of the wave-vector geometry for the chiral order parameter $\Delta(\mathbf{k})=e^{i\phi}\sin(ck_3)$. Here, k_3 is along the vertical axis. Note that the transmitted holelike and electronlike quasiparticles have the same value of the phase ϕ, so that no additional phase is introduced by the chiral factor and the results are identical to the $\sin(ck_3)$ case.

We note that the last two order parameters are odd under reflection around the basal plane; for all order parameters, this reflection is equivalent to replacing θ in Figs. 2 and 3 and the above equations by $\pi-\theta$ (note that this is equivalent to reflection around $\theta=\pi/2$). This is immediately apparent for $\sin ck_3$, and the geometric diagram in Fig. 4 shows that it is true for $\exp(i\phi)\sin ck_3$. Hence, when the tunneling is along the k_3 axis, this sign change is expected to produce ZBCPs (Ref. 10) in the tunneling conductance. We will see that this is indeed the case.

V. RESULTS

Figure 5 presents the normalized differential conductance dI/dV for the four order parameters described above, for the case where the tunneling direction is along the c axis, the normal metal is lead, and $T \ll T_c$. These are the conditions of the experimental data at $T=0.3$ K by Jourdan *et al.*[1] We have taken here the broadening factor Γ to be 54 μeV, which compares well with that extracted from de Haas–van Alphen measurements,[26] which measured Dingle temperatures of 0.1–0.28 K, corresponding to $\Gamma=27-76$ μeV. We find excellent agreement with the data of Jourdan *et al.*[1] throughout the whole range modeled for the order parameters $\cos(ck_3)$ and $\cos(2ck_3)$, while contrary to experiment, a ZBCP is predicted for the two sine-containing order parameters. Based on these data, we thus believe that it is rather unlikely that either of these two order parameters is relevant for UPd_2Al_3, although based upon calculations by Nishikawa and Yamada[30] the $\sin(ck_3)$ gap function may have relevance for the isostructural superconductor UNi_2Al_3. This material has indeed been proposed as a triplet superconductor having an odd gap function.[31]

For completeness, we have computed dI/dV in the transverse direction, where the tunneling current is in the basal

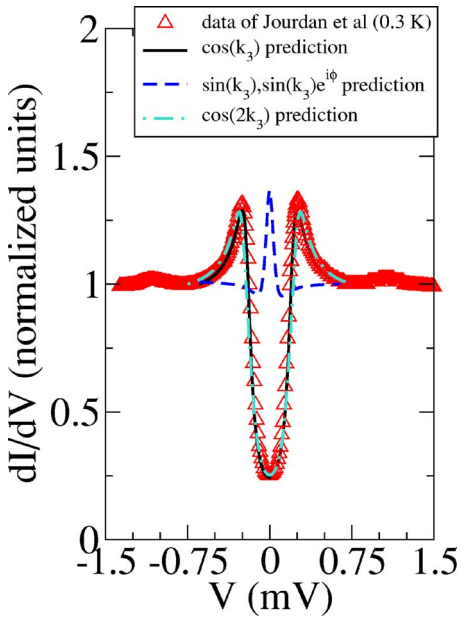

FIG. 5. (Color online) The tunneling data of Jourdan *et al.* at 0.3 K, with lead as the normal metal, are compared with predictions for the four order parameters shown.

plane, with the same parameters as above. The results are shown in Fig. 6. As in the first plot, there is little difference between the two cosine order parameters, while the $\sin(ck_3)$ result shows virtually no coherence peak and no ZBCP, but a high zero-energy density of states (ZDOS). This is a direct result of the selected angle of incidence for lead in this geometry falling very near the nodal line for this order parameter; this property will be used to full advantage in proposing an experiment to distinguish between the two cosine order parameters. We have also performed calculations for the $\cos(ck_3)$ gap function for the entire range of temperatures tested by Jourdan *et al.*, from 0.3–1.5 K (in this experiment,

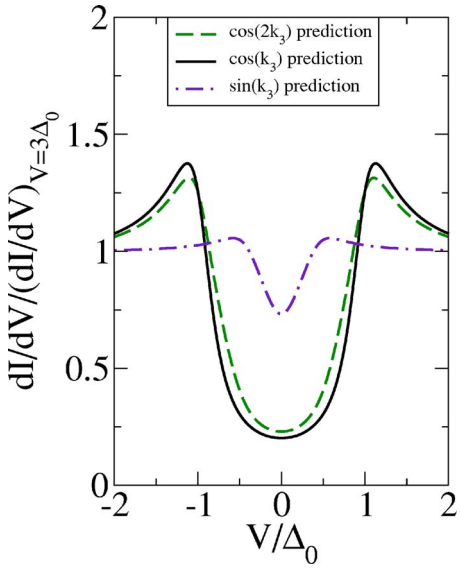

FIG. 6. (Color online) The predictions for the *ab*-plane tunneling conductance for the three order parameters indicated are shown.

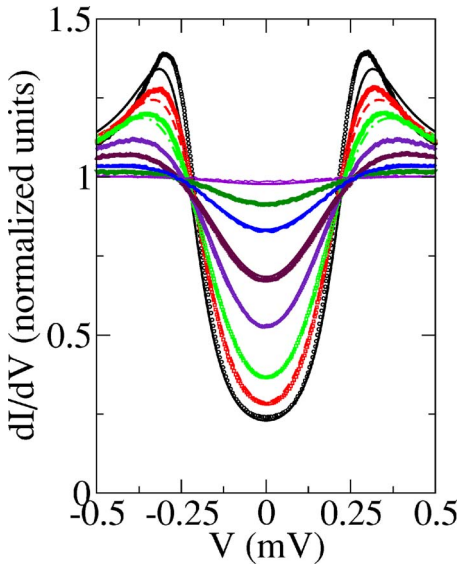

FIG. 7. (Color online) The fits to the data of Jourdan *et al.* using the $\cos(ck_3)$ order parameter are shown.

T_c was 1.6 K). Figure 7 shows excellent agreement with this order parameter over the entire temperature range, for nearly all energies. We stress that this was accomplished with a minimum of fitting parameters; the Dynes parameter Γ was assumed temperature independent (=54 μV) and the maximum energy gap value $\Delta(T)$ for all temperatures was near the value appropriate for BCS weak-coupling superconductors of this pairing symmetry.[32,33] We have plotted in Fig. 8 the fitted values of $\Delta(T)$ compared to the BCS prediction. We note that based upon the fits of these data, the ratio $2\Delta(0)/T_c$ is approximately 3.7, indicating that a weak-coupling treatment may be accurate for this calculation. For this order parameter, in the weak-coupling limit the ratio $2\Delta(0)/T_c$ is 4.3. We also note, however, the slight bump in the data of Jourdan *et al.* in Fig. 5 around $V=1$ mV, which may be indicative of strong coupling to a magnetic-exciton boson.[27,34]

We have not performed detailed comparison with experiment for the $\cos(2ck_3)$ order parameter, although it is quite possible that similar agreement with experiment could be obtained for this case. We believe that this order parameter

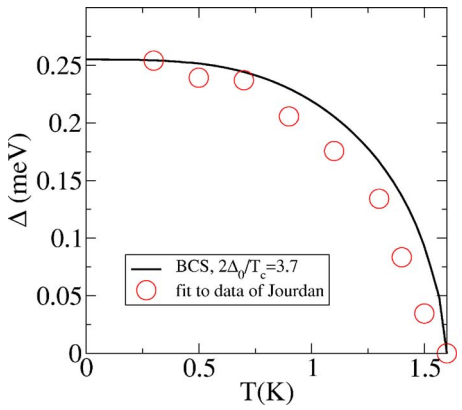

FIG. 8. (Color online) The fitted values of $\Delta(T)$ are shown.

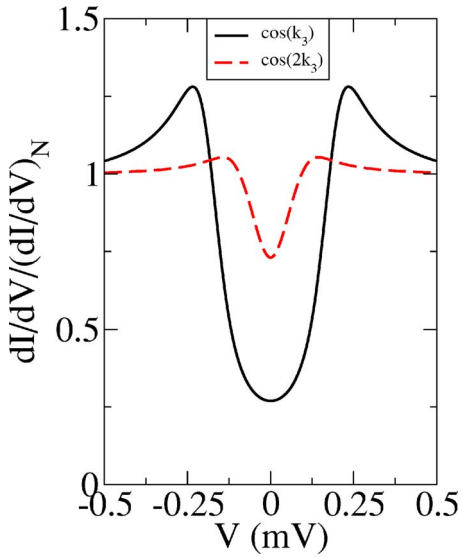

FIG. 9. (Color online) Predictions for the c-axis N-S tunneling with calcium as the normal metal are shown.

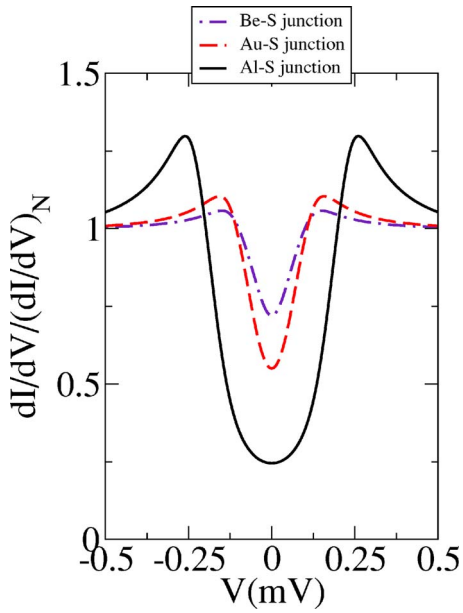

FIG. 10. (Color online) Predictions for the c-axis N-S tunneling for $\cos(ck_3)$ with beryllium, gold, and aluminum as the normal metals are shown.

may be less likely to apply for UPd_2Al_3 for the reasons presented in Ref. 34; namely, the formation of a resonance peak in inelastic neutron scattering[35] requires, in the magnetic-exciton scenario, a sign change over points on the Fermi surface separated by the antiferromagnetic wave vector $\mathbf{q}=\frac{\pi}{c}\hat{k}_3$ and this does not apply for this order parameter. Nevertheless, we have devised what we believe is a definitive experiment to finally determine the order parameter in UPd_2Al_3 after 15 years (Ref. 2) of study.

VI. PROPOSED EXPERIMENT: ORDER-PARAMETER DETERMINATION

The proposed experiment makes use of the unusual Fermi-surface geometry effects present for tunneling in the c-axis direction. The matching of wave vectors in the metal and in UPd_2Al_3 places sharp constraints on which region of the UPd_2Al_3 Fermi surface is employed by the superconducting electrons. In particular, it is possible to choose the normal metal so that for the $\cos(2ck_3)$ order parameter, the selected wave vector lies very near the nodal line, while for the $\cos(ck_3)$ order parameter, the selected wave vector is much more distant from the nearest node. We have chosen calcium for this purpose as its Fermi wave vector, based on a spherical-Fermi-surface approximation,[36] lies very near a nodal line of $\cos(2ck_3)$ but is far from a nodal line of $\cos(ck_3)$. The same situation would apply for thallium and cesium, but these are soft and reactive metals[37] that are not likely to be useful in forming a tunnel junction.

In Fig. 9, we show the results of the calculation for calcium at $T=0$, with the same quasiparticle lifetime broadening factor as before. We observe that for the $\cos(ck_3)$ case, reasonably well-developed coherence peaks, at a magnitude of approximately 250 μV, and a comparatively low ZDOS ($\simeq 0.25$) are present. However, for the $\cos(2ck_3)$ case, the coherence peaks are much broader and occur at significantly lower bias voltages ($V \simeq 150$ μV). In addition, the ZDOS is much higher, approximately 0.75. These differences are sufficiently robust that we believe that a calcium-based tunnel junction experiment, if technically feasible, would be sufficient to distinguish between these two order parameters. We recognize the inherent difficulty in forming a tunnel junction with a metal as reactive as calcium. However, its Fermi wave vector is virtually optimal for order-parameter determination; no other metal has a Fermi wave vector so near a nodal line of $\cos(2ck_3)$ but far from a nodal line of $\cos(ck_3)$. We therefore believe that the importance of such an experiment justifies substantial efforts to perform it, despite its difficulty.

For a final experiment of interest, we have computed the $T=0$ conductance for the $\cos(k_3)$ case for three metals commonly used in tunneling experiments—beryllium, gold, and aluminum—and show the results in Fig. 10. As in the previous plot, the coherence peak height and energy vary greatly from one metal to another, with concomitant variations in the ZDOS. We believe that such experiments would be a good validation of the basic model employed in this paper, and would provide useful information regarding the assumption that only very few states on the UPd_2Al_3 Fermi surface contribute to the tunneling conductance.

VII. CONCLUSION

We have analyzed the tunneling spectroscopy of the heavy-fermion superconductor UPd_2Al_3 and studied four possible gap functions for this material: $\cos(ck_3)$, $\cos(2ck_3)$, $\sin(ck_3)$, and $\exp(i\phi)\sin(ck_3)$. We find that the last two gap functions would be expected to show zero-bias conductance peaks in c-axis tunneling experiments as performed by Jourdan *et al.*;[1] these peaks were not observed and therefore these order parameters can be excluded. We further find that the

$\cos(ck_3)$ order parameter gives an excellent fit to the experimental data of Jourdan *et al.* at all temperatures, with a minimum of fitting parameters and a $\Delta(T)$ appropriate for the weak-coupling BCS theory of this material. Finally, we propose a definitive experiment to distinguish between the $\cos(ck_3)$ and $\cos(2ck_3)$ order parameters.

[1] M. Jourdan, M. Huth, and H. Adrian, Nature (London) **398**, 47 (1999).

[2] C. Geibel, C. Schank, S. Thies, H. Kitazawa, C. D. Bredl, A. Böhm, M. Rau, A. Grauel, R. Caspary, R. Helfrich, U. Ahlheim, G. Weber, and F. Steglich, Z. Phys. B: Condens. Matter **84**, 1 (1991).

[3] R. Feyerherm, A. Amato, F. N. Gygax, A. Schenck, C. Geibel, F. Steglich, N. Sato, and T. Komatsubara, Phys. Rev. Lett. **73**, 1849 (1994).

[4] H. Tou, Y. Kitaoka, K. Asayama, C. Geibel, C. Schank, and F. Steglich, J. Phys. Soc. Jpn. **64**, 725 (1995).

[5] K. Matsuda, Y. Kohori, and T. Kohara, Phys. Rev. B **55**, 15223 (1997).

[6] M. Hiroi, M. Sera, N. Kobayashi, Y. Haga, E. Yamamoto, and Y. Onuki, J. Phys. Soc. Jpn. **66**, 1595 (1997).

[7] T. Watanabe, K. Izawa, Y. Kasahara, Y. Haga, Y. Onuki, P. Thalmeier, K. Maki, and Y. Matsuda, Phys. Rev. B **70**, 184502 (2004).

[8] G. E. Blonder, M. Tinkham, and T. M. Klapwijk, Phys. Rev. B **25**, 4515 (1982).

[9] A. F. Andreev, Sov. Phys. JETP **19**, 1228 (1964).

[10] Y. Tanaka and S. Kashiwaya, Phys. Rev. Lett. **74**, 3451 (1995).

[11] J. Y. T. Wei, N.-C. Yeh, D. F. Garrigus, and M. Strasik, Phys. Rev. Lett. **81**, 2542 (1998).

[12] M. Tinkham, *Introduction to Superconductivity*, 2nd ed. (Dover, New York, 2004).

[13] C. Honerkamp and M. Sigrist, J. Low Temp. Phys. **111**, 895 (1998).

[14] P. G. deGennes, *Superconductivity of Metals and Alloys* (Addison-Wesley, Reading, MA, 1989).

[15] T. M. Klapwijk, G. E. Blonder, and M. Tinkham, Physica B & C **109–110**, 1657 (1982).

[16] A. A. Abrikosov and L. P. Gor'kov, Sov. Phys. JETP **12**, 1243 (1961).

[17] N. E. Hussey, Adv. Phys. **51**, 1685 (2002).

[18] P. J. Hirschfeld, P. Wölfle, and D. Einzel, Phys. Rev. B **37**, 83 (1988).

[19] R. C. Dynes, V. Narayanamurti, and J. P. Garno, Phys. Rev. Lett. **41**, 1509 (1978).

[20] D. A. Browne, K. Levin, and K. A. Muttalib, Phys. Rev. Lett. **58**, 156 (1987).

[21] T. P. Devereaux and D. Belitz, J. Low Temp. Phys. **77**, 319 (1989).

[22] J. R. Schrieffer, *Theory of Superconductivity* (Perseus, Reading, 1999).

[23] A. Pleceník, M. Grajcar, Š. Beňačka, P. Seidel, and A. Pfuch, Phys. Rev. B **49**, 10016 (1994).

[24] M. Grajcar, A. Pleceník, P. Seidel, and A. Pfuch, Phys. Rev. B **51**, 16185 (1995).

[25] K. Sengupta, I. Žutić, H. J. Kwon, V. M. Yakovenko, and S. Das Sarma, Phys. Rev. B **63**, 144531 (2001).

[26] Y. Inada, H. Aono, A. Ishiguro, J. Kimura, N. Sato, A. Sawada, and T. Komatsubara, Physica B **119**, 119 (1994); Y. Inada, A. Ishiguro, J. Kimura, N. Sato, A. Sawada, T. Komatsubara, and H. Yamagami, *ibid.* **206–207**, 33 (1995); Y. Inada, H. Yamagami, Y. Haga, K. Sakurai, Y. Tokiwa, T. Honma, E. Yamamoto, Y. Onuki, and T. Yanagisawa, J. Phys. Soc. Jpn. **68**, 3643 (1999).

[27] P. McHale, P. Fulde, and P. Thalmeier, Phys. Rev. B **70**, 014513 (2004).

[28] Y. Matsuda, K. Izawa, and I. Vekhter, J. Phys.: Condens. Matter **18**, R705 (2006).

[29] H. Won, D. Parker, K. Maki, T. Watanabe, K. Izawa, and Y. Matsuda, Phys. Rev. B **70**, 140509(R) (2004).

[30] Y. Nishikawa and K. Yamada, J. Phys. Soc. Jpn. **71**, 2629 (2002).

[31] K. Ishida, D. Ozaki, T. Kamatsuka, H. Tou, M. Kyogaku, Y. Kitaoka, N. Tateiwa, N. K. Sato, N. Aso, C. Geibel, and F. Steglich, Phys. Rev. Lett. **89**, 037002 (2002).

[32] We note that the temperature dependence of the gap in the weak-coupling approximation is the same as for *d*-wave superconductors, as the Fermi-surface angular averages $\langle f^2 \rangle$ and $\langle f^2 \ln|f| \rangle$, where $\Delta(\mathbf{k}) = \Delta(T) f(\mathbf{k})$, are identical. See Ref. 33.

[33] H. Won and K. Maki, Phys. Rev. B **49**, 1397 (1994).

[34] J. Chang, I. Eremin, P. Thalmeier, and P. Fulde, Phys. Rev. B **75**, 024503 (2007).

[35] N. K. Sato, N. Aso, K. Miyake, R. Shiina, P. Thalmeier, G. Varelogiannis, C. Geibel, F. Steglich, P. Fulde, and T. Komatsubara, Nature (London) **410**, 340 (2001).

[36] N. W. Ashcroft and N. D. Mermin, *Solid State Physics* (Thomson Learning, Singapore, 1976).

[37] *Handbook of Chemistry and Physics*, 2nd ed., edited by D. R. Lide (CRC, Boca Raton, 1996).